Journal of
Mechanical
Science and
Technology

Journal of Mechanical Science and Technology 21 (2007) 1196~1206

Intelligent Phase Plane Switching Control of a Pneumatic Muscle Robot Arm with Magneto-Rheological Brake

Kyoung Kwan Ahn[a,*], Nguyen Huynh Thai Chau[b]

[a]*School of Mechanical and Automotive Engineering, University of Ulsan, San 29, Muger 2dong, Nam-gu, Ulsan, 680-764, Korea*
[b]*Graduate School of Mechanical and Automotive Engineering, University of Ulsan*

(Manuscript Received July 3, 2006; Revised April 27, 2007; Accepted April 27, 2007)

Abstract

Pneumatic cylinders are one kind of low cost actuation sources which have been applied in industrial and robotics field, since they have a high power/weight ratio, a high-tension force and a long durability. To overcome the shortcomings of conventional pneumatic cylinders, a number of newer pneumatic actuators have been developed such as McKibben Muscle, Rubber Actuator and Pneumatic Artificial Muscle (PAM) Manipulators. However, some limitations still exist, such as the air compressibility and the lack of damping ability of the actuator bring the dynamic delay of the pressure response and cause the oscillatory motion. In addition, the nonlinearities in the PAM manipulator still limit the controllability. Therefore, it is not easy to realize motion with high accuracy and high speed and with respect to various external inertia loads.

To overcome these problems, a novel controller which harmonizes a phase plane switching control method (PPSC) with conventional PID controller and the adaptabilities of neural network is newly proposed. In order to realize satisfactory control performance a variable damper, Magneto-Rheological Brake (MRB), is equipped to the joint of the robot. The mixture of conventional PID controller and an intelligent phase plane switching control using neural network (IPPSC) brings us a novel controller. The experiments were carried out in a robot arm, which is driven by two PAM actuators, and the effectiveness of the proposed control algorithm was demonstrated through experiments, which had proved that the stability of the manipulator can be improved greatly in a high gain control by using MRB with IPPSC and without regard for the changes of external inertia loads.

Keywords: Pneumatic artificial muscle; Neural network; Intelligent control; Magneto-rheological brake; Phase plane switching control; Pneumatic robot arm

1. Introduction

Industrial robots have been used three primary types of actuator: electric motor (DC or AC), hydraulic cylinders and pneumatic cylinders. Their performance is characterized by parameters such as power/weight ratio, strength, response rate, physical size, speed of motion, reliability, controllability, compliance, cost and so on. Most robotic manipulators today adapt electric drives in the form of servomotors or stepping motors, but the disadvantages of electrical systems are low power, low torque/weight ratio and the possibility of sparking. Although hydraulic actuators are used for high-speed operation, their main drawback lies in the lack of cleanliness. Therefore, pneumatic actuators are finding increased use in robotic systems due to cheapness, quickness of response, high power/weight and power/volume ratios. However, they have not been widely applied in advanced robotics due to two interrelated problem: the accuracy and difficulty of

*Corresponding author. Tel.: +82 52 259 2282, Fax.: +82 52 259 1680
E-mail address: kkahn@ulsan.ac.kr

control and compliance (sponginess), which means that load variations have a significant effect on the position control.

A novel actuator, which has been regarded during the recent decades as an interesting alternative to hydraulic and electric actuators, is pneumatic artificial muscle. It is superior to other actuators such as electric motor and pneumatic cylinder in the safety for human because of flexibility and the lightness, of which property is preferable in contacting tasks with human.

Fortunately, the development of novel actuators such as the McKibben Muscle, Rubber Actuator and Pneumatic Artificial Muscle (PAM) Manipulators satisfied the requirements of advanced robotic construction. PAM is able to exhibit many of the properties found in the real biological muscle. Contrary to its simple design, the control of PAM is very complex due to its nonlinearity, compressibility of air, oscillatory motion, time varying properties, and difficulties in analytical modeling. Therefore, it is not easy to realize motion with high accuracy, high speed and with respect to various external loads.

As a result, a considerable amount of research has been devoted to the development of various position control systems for the PAM manipulator. The discrete time PID controllers with a feedforward term were implemented for controlling a pneumatic muscle (Caldwell et al., 1993). This controller was turned by trial and error to yield a suitable closed-loop bandwidth with a little overshoot. Static and dynamic mathematical models of PAM actuator had been done by Colbrunn and his colleagues (2001). These models can be extended beyond large-scale biorobot from the simulation results of this paper. For bi-muscular PAM systems, the adaptive pole placement controller was proposed with the accurate position control ±2° (Medrano-Cerda et al., 1995). In addition, a Kohonen-type neural network was used for position control of the robot end-effector within 1 cm after learning (Hesselroth et al., 1994). Recently, Van der Smagt et al. (1996) have developed a feedforward neural network controller, where the joint angle and pressure of each chamber of the pneumatic muscle were used as learning data and the accurate trajectory following was obtained.

Nowadays, robots play an important role in industry. They can replace the human actions in highly hazardous places especially in the processes of nuclear clean-up, dismantling and decontamination (Caldwell et al., 1999). Therefore, for widespread use of these actuators in the robotic field, a high speed and accurate control of the PAM manipulators is required. PID control (Tsagarakis et al., 1999), fuzzy PD+I learning control (Chan et al., 2003), sliding mode control (Tondu et al., 2000; Carbonell et al., 2001), H infinity control (Osuka et al., 1990; Ahn et al., 2003), feedforward control + fuzzy logic (Kishore et al., 2003), adaptive control (Caldwell et al., 1995; Medrano-Cerda et al., 1995) and so on, have been applied to control the PAM manipulator. Though these systems were successful in addressing smooth actuator motion in response to step inputs, the external inertia load were also assumed to be constant or slowly varying. In industrial fields, due to the requirements of productivity, the robot arm is necessary to realize the fast response and high accuracy even if the external inertia load changes severely. Therefore, it is necessary to propose a new control algorithm, which is applicable to a very compressible PAM system with various loads.

Intelligent control techniques have emerged to overcome some deficiencies in conventional control methods in dealing with complex real-world systems such as PAM manipulator. Many new control algorithms based on a neural network have been proposed. An intelligent control using a neuro-fuzzy network was proposed by Iskarous et al. (1995). A hybrid network that combines fuzzy and neural network was used to model and control complex dynamic systems, such as the PAM system. An adaptive controller based on the neural network was applied to the artificial hand, which is composed of the PAM (Folgheraiter et al., 2003). Here, the neural network was used as a controller, which had the form of compensator or inverse of the model and it was not easy to apply these control algorithms to the greatly changing inertia load systems. In addition, these control algorithms were not yet to reconcile both damping and response speed in high gain control.

To overcome these problems, a new technology, Electro-Rheological Fluid Damper (ER Damper), has been applied to the PAM manipulator. Noritsugu et al. (1997) have used ER damper to improve the control performance of the PAM manipulator with PI controller and pulse code modulated on-off valves. By separating the region where the damper produces a damping torque in order to reconcile both damping and response speed in high gain control, the results show that the ER damper is one of effective methods

Table 1. Comparison of rheological fluids.

	Magneto-Rheological Fluid	Electro-Rheological Fluid
Max. Yield Stress	50 –100 kPa	2 – 5 kPa
Viscosity	0.1 – 1.0 Pa-s	0.1 – 1.0 Pa-s
Operable Temp. Range	-40 to + 150 °C	+10 to + 90 °C (ionic, DC) -25 to + 125 °C (non-ionic, AC)
Stability	Unaffected by most impurities	Cannot tolerate impurities
Response Time	< milliseconds	< milliseconds
Density	3 – 4 g/cm^3	1 – 2 g/cm^3
Max. Energy Density	0.1 Joule/cm^3	0.001 Joule/cm^3
Power Supply	2 – 25 V @ 1 – 2 A (2 – 50 watts)	2 – 25 KV @ 1 – 10 mA (2 – 50 watts)

to improve the performance of position control without the decrease of response speed. However, some limitations still exist, such as ER Fluid (ERF) requires extremely high control voltage (kV) which is problematical and potentially dangerous, only operates in a narrow range of temperature which can not be applied for PAM manipulator, and has also the characteristics of nonlinearity. In recent years, because ERF has many unacceptable disadvantages, Magneto-Rheological Fluid (MRF) attracts people's attention with these advantages in Table 1.

The object of this paper is to implement pneumatic artificial muscle and MRB to develop a fast, accurate response and position control of pneumatic muscle robot arm by IPPSC taking account of the changes of external loads. The experiments were carried out in practical pneumatic muscle robot arm and the effectiveness of the proposed control algorithm was demonstrated through experiments, which had proved that the stability of the manipulator can be well improved in a high gain control by using MRB with IPPSC and without decreasing the response speed and low stiffness of manipulator.

2. Experimental setup

2.1 Experimental apparatus

The schematic diagram of the robot arm using pneumatic artificial muscle is shown in Fig. 1. The hardware includes an IBM-compatible personal computer (Pentium 1 GHz), which calculated the control input and controlled the proportional valve

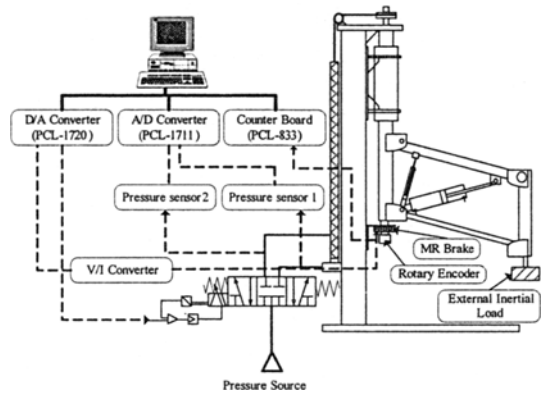

Fig. 1. Schematic diagram of the robot arm using pneumatic artificial muscle.

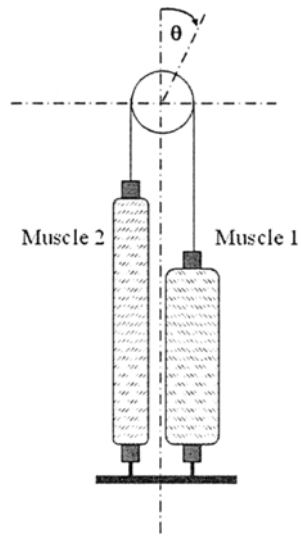

Fig. 2. Antagonistic muscle scheme.

(FESTO, MPYE-5-1/8HF-710 B) and Magneto-Rheological Brake (LORD, MRB-2107-3 Rotary Brake), through D/A board (Advantech, PCI 1720), and MRB is controlled by D/A broad through voltage to current converter, Wonder Box Device Controller Kit (LORD, RD-3002-03). The antagonistic muscle (FESTO, MAS-10-N-220-AA-MCFK) scheme is shown in Fig. 2. The two muscles are connected by a chain across a sprocket, and when different air pressures are supplied to a muscle, the different equilibrium lengths result in a change of the equilibrium angle for the joint angle. A joint angle θ and the air pressure in each muscle were measured by a rotary encoder (METRONIX, H40-8-3600ZO) and the pressure sensors (FESTO, SDE-10-10). These signals feed back to the computer through a 24-bit

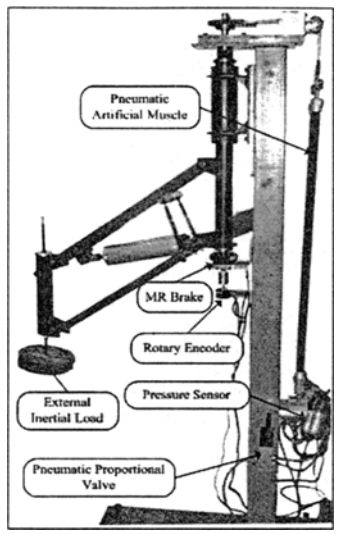

Fig. 3. Photograph of the experimental apparatus.

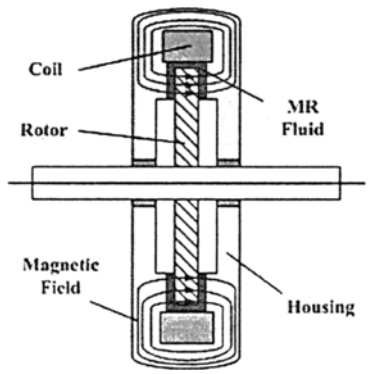

Fig. 4. Construction of MRB.

digital counter board (Advantech, PCL 833) and A/D board (Advantech, PCI 1711), respectively. The load could be changed from no load to 10 Kg. The experiments were conducted in 5 [bar] and all control software was coded in C program language. A photograph of the experimental apparatus is shown in Fig. 3.

2.2 Characteristics of MRB

Construction of MRB was shown in Fig. 4. The rotor in Fig. 4 is fixed to the shaft, which can rotate in relation to housing. Between rotor and housing there is a gap filled with MRF. Braking torque of MRB can be controlled by the electric current in its coil. An apparent viscosity of MRF is changed at few milliseconds after the application of a magnetic field, and goes back to the normal viscosity with no magnetic field.

Table 2. Measurement data of MRB.

W / I	0	0.1	0.2	0.3	0.4	0.5	0.6	0.7	0.8	0.9	1
100	0.28	0.81	1.33	1.87	2.44	2.93	3.51	4.03	4.5	5.11	5.57
200	0.31	0.82	1.33	1.92	2.4	2.96	3.57	3.99	4.54	5.12	5.67
300	0.3	0.81	1.36	1.89	2.48	2.99	3.54	4.03	4.55	5.13	5.58
400	0.31	0.82	1.35	1.94	2.46	2.98	3.55	4.05	4.59	5.05	5.62
500	0.31	0.83	1.37	1.87	2.4	2.99	3.55	4.08	4.61	5.06	5.58
600	0.3	0.83	1.36	1.87	2.48	3	3.53	4.05	4.54	5.06	5.55
700	0.28	0.86	1.37	1.9	2.46	3.01	3.54	4.03	4.55	5.04	5.55
800	0.29	0.86	1.37	1.9	2.44	3.05	3.54	4.08	4.59	5.04	5.58
900	0.29	0.89	1.41	1.92	2.53	3.05	3.57	4.11	4.58	5.01	5.61
1000	0.29	0.89	1.44	1.93	2.53	3.04	3.57	4.14	4.61	5.03	5.59

W: Rotational Speed [rpm]
I: Current Applied [A]

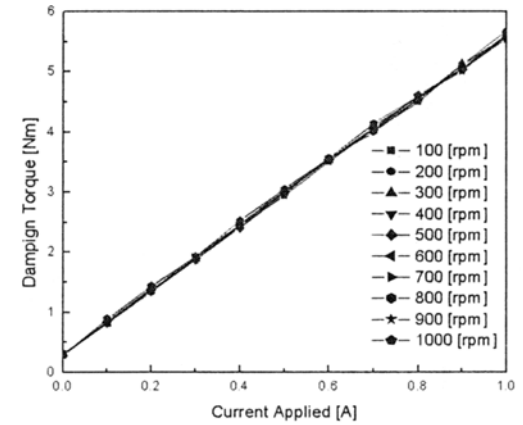

(a)

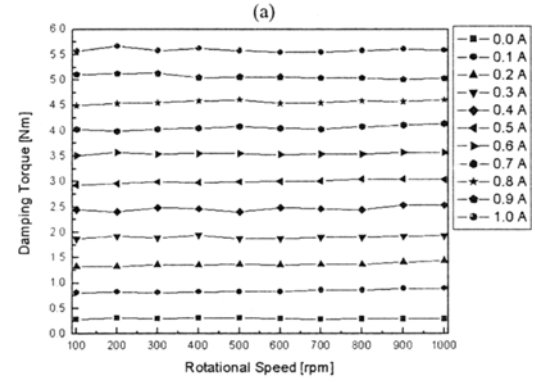

(b)

Fig. 5. Characteristics of MRB.

The following experiments are performed to investigate the characteristics of MRB, which measurement data is shown in Fig. 5 and Table 2.

MRB is connected with a torque transducer and a servomotor in series. In the experiments, the rotational speed is changed from 100 [rpm] to 1000 [rpm] and the current applied for MRB is changed from 0 [A] to 1[A]. The reason for choosing this range of rotational speed and current is that the response of system does not reach to 1000 [rpm] and the maximum current applied for MRB is 1 [A]. Figure 5 shows the damping torque with respect to the change of the input current (a) and rotational speed (b) of MR Brake. From Fig. 5, it is clear that the damping torque of MRB is independent of rotational speed and almost proportional to input current. Thus an Eq. (1) holds between the inputs current I and damping torque T_b

$$T_b = f(I) = a + bI \tag{1}$$

Here, a and b are constant.

3. Control system

3.1 Positioning control system

To control the robot arm using PAM actuator a conventional PID control algorithm is applied in this paper as the basic controller. The controller output can be expressed in the time domain as:

$$u(t) = K_p e(t) + \frac{K_p}{T_i}\int_0^t e(t)dt + K_p T_d \frac{de(t)}{dt} \tag{2}$$

A typical real-time implementation at sampling sequence k can be expressed as:

$$u(k) = K_p e(k) + u(k-1) + \frac{K_p T}{T_i} e(k) + K_p T_d \frac{e(k) - e(k-1)}{T} \tag{3}$$

where $u(k)$ and $e(k)$ are the control input to the control valve and the error between the desired set point and the output of joint, respectively.

In addition, MRB is one of effective methods to improve the control performance of the PAM manipulator by reconciling both the damping and response speed because it works in only the regions where the acceleration or deceleration is too high. Here, s is Laplace operator, T_a is torque produced by manipulator, T_c is constant torque and K_{ED} determines a

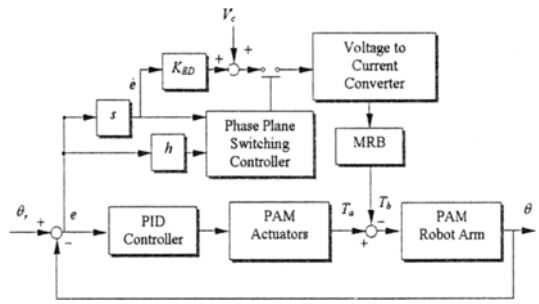

Fig. 6. Block diagram of PPSC.

gain for the torque proportional to the angular speed $\dot{\theta}$, V_c is a control voltage of source calculated from Eq. (1) to produce T_c. A direction of a damping torque is every time opposite to the rotary direction of the arm. So Eq. (4) below indicates that the damper produces a torque T_b.

$$T_b = \left(K_{ED}\dot{\theta} + T_c\right) sign(\dot{\theta}) \tag{4}$$

The structure of the proposed phase plane switching control method is shown in Fig. 6.

3.2 Conventional Phase Plane Switching Control method (PPSC)

The damping torque T_b improves the damping performance of the manipulator. Since the damping torque every time acts in the direction against the rotational direction of manipulator, its acceleration performance is degraded. In the region that the joint angle of the arm approaches to the desired angle, a~b, c~d in Fig. 7(a), the current is not applied not to interfere the movement of the arm, since the high response speed is required. In the region the arm passes the desired angle, i.e. the diagonally shaded areas of b~c, d~e in Fig. 7(a), a current is applied to improve the damping performance to converge to the desired angle quickly. To determine whether the magnetic field should be applied or not, the phase plane shown in Fig. 7(b) is used. The horizontal axis in the phase plane corresponds to joint angle deviation e between the desired angle θ_r and the joint angle θ, and the vertical axis corresponds to the derivation of the deviation $\dot{e} = \frac{de}{dt} = -\dot{\theta}$. Each point a~e on the phase plane corresponds to each point a~e in Fig. 7(a). Here, the regions with the application of current are controlled by h[s^{-1}], the gradient of the line shown in Fig. 7(b). The region under the application of the damping torque expands as $|h|$ decrease.

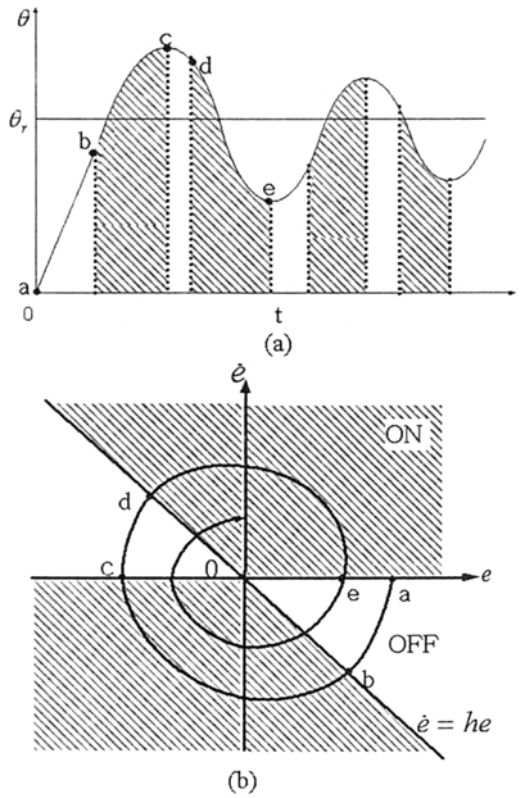

Fig. 7. Concept of PPSC.

3.3 Experimental results of PPSC

To discuss the effect of PPSC in the improvement of the control performance of pneumatic muscle robot arm, experiments for step responses are conducted. Figure 8 show the responses of the robot arm by PID control with various gains (PID controller 1: $K_P = 0.000009$; $K_I = 0.0000001$; $K_D = 0.000015$; PID controller 2: $K_P = 0.00007$; $K_I = 0.0000001$; $K_D = 0.00002$). It is apparent that both control performance and damping effect are difficult to satisfy at the same time. The robot arm must be controlled slowly in order to have a good stability. On the contrast, the overshoot and oscillation are always included if one wants fast response. Therefore, PPSC with MRB is necessary and the responses are shown in Fig. 9 with PID controller 2, K_{ED}=0.5, T_C=0.3 and various h (-3; -5; -10). These parameters were obtained by trial-and-error through experiments. From these experimental results, it is understood that the settling time becomes very big in some value of design parameters of switching controller. To guarantee the control performance, the control parameters must be tuned adaptively and we proposed

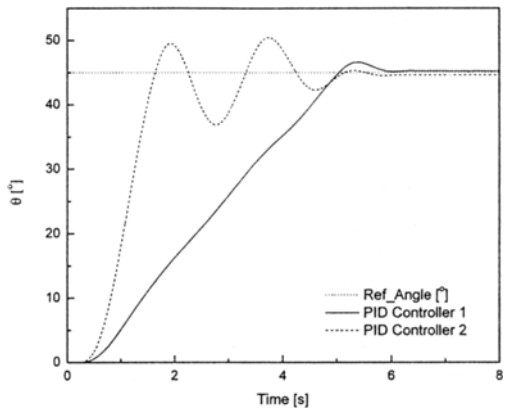

Fig. 8. Comparison between PID controller 1 and PID controller 2.

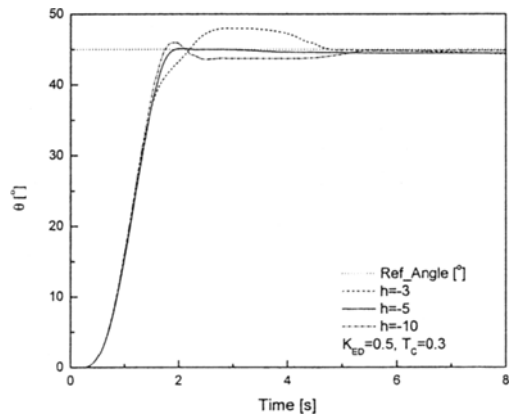

Fig. 9. Experimental results of PPSC with various parameter of *h*.

phase plane switching control with neural network newly, which is explained in detail in next section. All experiments with conventional phase plane switching control method were carried out by the condition ($K_{ED} = 0.5$, $T_c = 0.3$ *and* $h = -5$) of phase plane from now on.

4. Proposed Intelligent Phase Plane Switching Control using neural network (IPPSC)

4.1 Structure of IPPSC

From the experimental results, modification of control parameters of PPSC must be adjusted to realize more accurate control. It is obvious that the PPSC is limited because the K_{ED} parameter is constant. This means that the damping torque is not adaptable and optimal in any case. Here, we propose an intelligent phase plane switching control, which

has the adaptability of control parameter to minimize the position error. With the capacity of learning and adaptability of neural network, the proposed controller can solve these problems. The damping torque will be tuned adaptively and optimally in order to minimize the position error without respect to the variation of external inertia loads.

Figure 10 shows the structure of IPPSC. In Fig.10, the proportional gain K_{ED} in Fig. 6 was modified by neural network. The block diagram of neural network is shown in Fig. 11. Here $K_E(k)$, $K_{ED}(k)$, $e(k)$, $e_D(k)$, $x(k)$ and $f(x)$ are the proportional gain, the derivative gain, the system error between desired angle output and output of joint of the PAM manipulator, the difference of the system error, control input of MRB and sigmoid function of neural network, respectively. The sigmoid function, $f(x)$, which has a nonlinear relation is presented in the following equation:

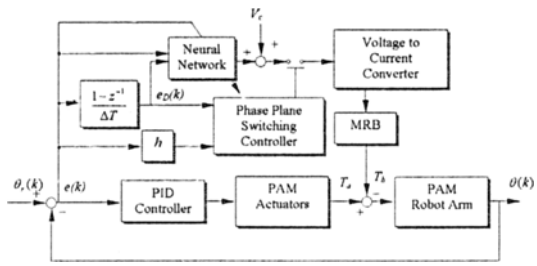

Fig. 10. The structure of IPPSC.

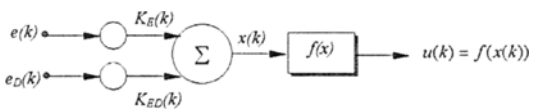

Fig. 11. The block diagram of neural network.

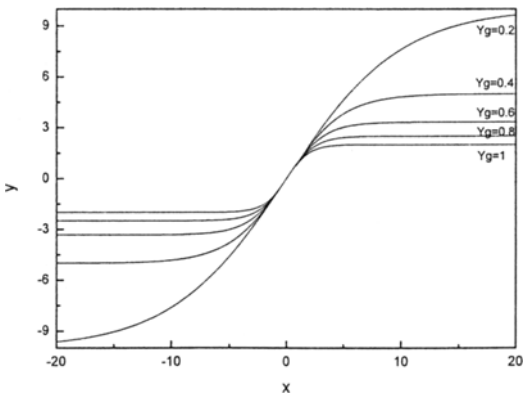

Fig. 12. The sigmoid function shapes.

$$f(x) = \frac{2(1 - e^{-xY_g})}{Y_g(1 + e^{-xY_g})} \tag{5}$$

where x is the input of sigmoid function and Y_g is the parameter determining its shape. Figure 12 shows the shapes of sigmoid function with various Y_g. As shown in Eq. (5), the sigmoid function $f(x)$ becomes linear when Y_g approaches zero.

We have two-layered nonlinear neurons. Neural networks are trained by the conventional back propagation algorithm to minimize the system error between the output of joint of the PAM manipulator and desired angle.

In Fig. 11, the input signal of the sigmoid function in the output layer, $x(k)$, becomes:

$$x(k) = K_E(k)e(k) + K_{ED}(k)e_D(k) \tag{6}$$

where,

$$e(k) = \theta_r(k) - \theta(k)$$
$$e_D(k) = \frac{e(k)(1 - z^{-1})}{\Delta T} \tag{7}$$

ΔT: sampling time, z: operator of Z-transform, K: discrete sequence

$\theta_r(k)$ and $\theta(k)$ are desired angle and output of joint of the PAM manipulator, respectively.

The damping torque of phase plane switching control using neural network can be obtained as the following equation:

$$T_h(k) = \left(f(x(k)) + T_c\right) sign(\dot{\theta}) \tag{8}$$

4.2 Learning algorithm of neural network

From Eq. (8), in order to get the optimal value of damping torque, the control parameters K_E and K_{ED} must be adjusted automatically in order to minimize the position error.

To tune K_E and K_{ED}, the steepest descent method using the following Eq. was applied.

$$K_E(k+1) = K_E(k) - \eta_E \frac{\partial E(k)}{\partial K_E}$$
$$K_{ED}(k+1) = K_{ED}(k) - \eta_{ED} \frac{\partial E(k)}{\partial K_{ED}} \tag{9}$$

where η_E and η_{ED} are learning rates determining convergence speed, and *E(k)* is the error defined by the following equation:

$$E(k)=\frac{1}{2}(\theta_r(k)-\theta(k))^2 \tag{10}$$

From Eq. (9), using the chain rule, we get the following equations:

$$\begin{aligned}\frac{\partial E(k)}{\partial K_E}&=\frac{\partial E(k)}{\partial \theta}\frac{\partial \theta(k)}{\partial u}\frac{\partial u(k)}{\partial x}\frac{\partial x(k)}{\partial K_E}\\ \frac{\partial E(k)}{\partial K_{ED}}&=\frac{\partial E(k)}{\partial \theta}\frac{\partial \theta(k)}{\partial u}\frac{\partial u(k)}{\partial x}\frac{\partial x(k)}{\partial K_{ED}}\end{aligned} \tag{11}$$

These following equations are derived by using Eqs. (6), (10):

$$\begin{aligned}&\frac{\partial E(k)}{\partial \theta}=-(\theta_r(k)-\theta(k))=-e(k)\\ &\frac{\partial u(k)}{\partial x}=f'(x(k))\\ &\frac{\partial x(k)}{\partial K_E}=e(k);\quad \frac{\partial x(k)}{\partial K_{ED}}=e_D(k)\end{aligned} \tag{12}$$

And the following expression can be derived from these Eqs. (11), (12).

$$\begin{aligned}\frac{\partial E(k)}{\partial K_E}&=\frac{\partial E(k)}{\partial \theta}\frac{\partial \theta(k)}{\partial u}\frac{\partial u(k)}{\partial x}\frac{\partial x(k)}{\partial K_E}\\ &=-e(k)\frac{\partial \theta(k)}{\partial u}f'(x(k))e(k)\\ &=-\frac{\partial \theta(k)}{\partial u}f'(x(k))e^2(k)\\ \frac{\partial E(k)}{\partial K_{ED}}&=\frac{\partial E(k)}{\partial \theta}\frac{\partial \theta(k)}{\partial u}\frac{\partial u(k)}{\partial x}\frac{\partial x(k)}{\partial K_{ED}}\\ &=-e(k)\frac{\partial \theta(k)}{\partial u}f'(x(k))e_D(k)\\ &=-\frac{\partial \theta(k)}{\partial u}f'(x(k))e(k)e_D(k)\end{aligned} \tag{13}$$

and $f'(x)=4\dfrac{e^{-x\cdot Yg}}{(1+e^{-x\cdot Yg})^2}$ (14)

As done by Yamada and Yabuta, for convenience, $\dfrac{\partial \theta(k)}{\partial u}=1$ is assumed. Then the Eq. (9) is expressed as follows:

$$\begin{aligned}K_E(k+1)&=K_E(k)+\eta_E e(k)e(k)\frac{4e^{-x\cdot Yg}}{(1+e^{-x\cdot Yg})^2}\\ K_{ED}(k+1)&=K_{ED}(k)+\eta_{ED}e(k)e_D(k)\frac{4e^{-x\cdot Yg}}{(1+e^{-x\cdot Yg})^2}\end{aligned} \tag{15}$$

The effectiveness of the proposed IPPSC with tuning algorithm of damping torque will be demonstrated through experimental results with various external inertia loads.

4.3 Experimental results

The experiments were carried out with 3 cases of external inertia loads (0, 5 and 10 Kg). The initial control parameters of IPPSC were set to be $T_c=0.3$, $h=-5$, $Y_g=0.3$, $K_E=0.1$, $K_{ED}=0.1$, $\eta_E=25\times10^{-7}$ and $\eta_{ED}=25\times10^{-8}$. These control parameters were obtained by trial-and-error through experiments. Thus, from now on, these control parameters were applied for the IPPSC in all case of experiments.

In Fig. 13, comparisons were made between the conventional PID controller, PPSC and IPPSC with respect to load condition 1 (No load). In the experiments, the joint angle of pneumatic muscle robot arm was in good agreement with that of reference by using PPSC. However it has too large settling time and more overshoot because of fixed parameters of switching controller. We have a very good performance of pneumatic muscle robot arm in the case of using IPPSC. It is clear that the newly proposed controller using neural network was effective in this experimental condition. The effectiveness of the proposed control algorithm with neural network was also shown in detail in Fig. 14. The damping torque was not applied for fast response when the robot arm starts to move and the damping torque was generated by MRB to the rotational axis of robot arm in order to reduce the overshoot and oscillation when the manipulator reaches the desired angle. In addition, during the experiment of pneumatic muscle robot arm, the control parameters K_E and K_{ED} was tuned adaptively by neural network to minimize the position error.

Next, experiments were executed to investigate the control performance with various external inertia loads. Figure 15 shows the comparison between the conventional PID controller, PPSC and IPPSC in the case of the load condition 2 (5 Kg). From the experi-

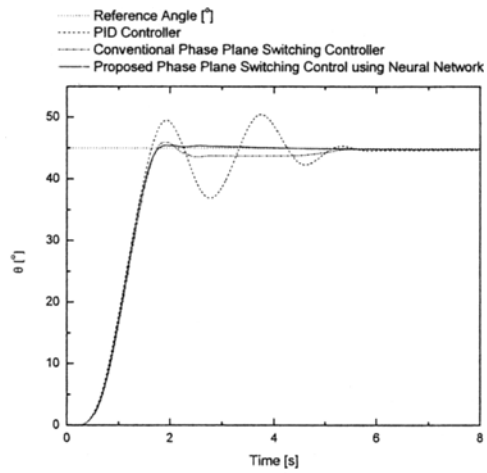

Fig. 13. Comparison between PID controller, PPSC and IPPSC. (Load condition 1)

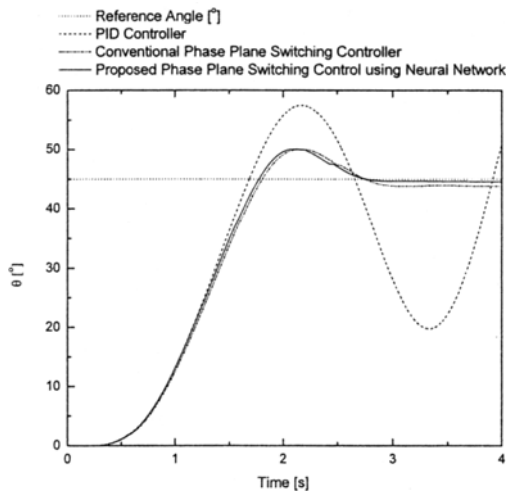

Fig. 15. Comparison between PID controller, PPSC and IPPSC. (Load condition 2)

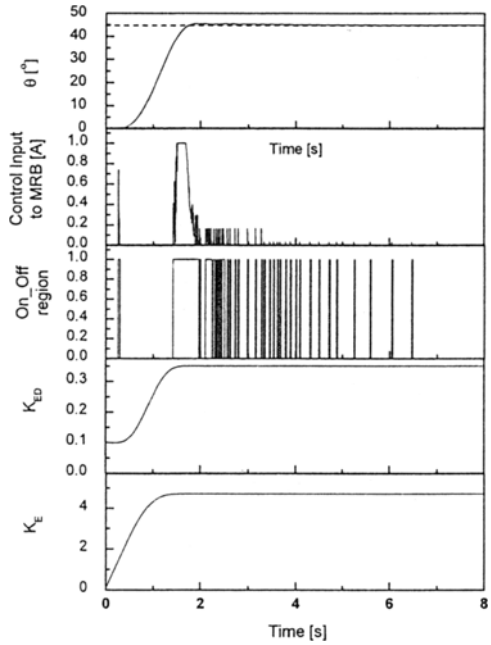

Fig. 14. Experimental results of IPPSC. (Load condition 1)

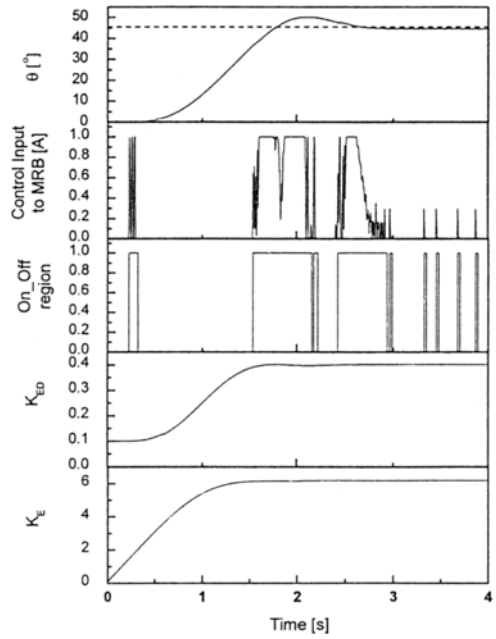

Fig. 16. Experimental results of IPPSC. (Load condition 2)

mental results, it was found that a good control performance, strong robustness with a little overshoot were obtained without respect to the variation of external inertia load by using IPPSC. In Fig. 16, the experimental result of IPPSC with external inertia load condition 2 was shown in detail. From these experimental results, the damping torque was applied and released very frequently according to the approach to the desired angle. It was demonstrated that the proposed algorithm was effective in the case of various external inertia loads.

In order to demonstrate the proposed IPPSC, the external inertia load was changed from 0, 5 and 10Kg, respectively. Experiments were conducted to compare the system response of PID controller, PPSC and IPPSC under the external load condition 3 (10 Kg) in Fig. 17. With up to 10 Kg bigger external inertia load with respect to the minimum external inertia load, the responses of PID controller and PPSC are oscillated due to the fixed control parameter. However, with

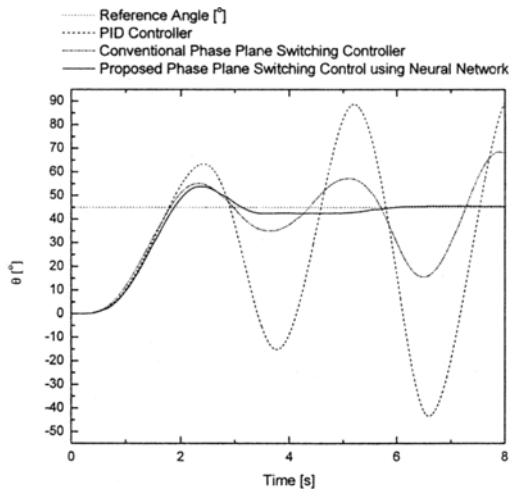

Fig. 17. Comparison between PID controller, PPSC and IPPSC. (Load condition 3)

newly proposed IPPSC, the good control performance was obtained. Figure 18 shows the experimental results of IPPSC in detail with respect to the external inertia load condition 3. It was concluded that the proposed controller was very effective in the high gain control, good control performance, fast response, and strong robust stability with respect to the large external inertia load variation (0 to 10 Kg).

5. Conclusions

In this paper, a newly proposed phase plane switching control using neural network was applied to the pneumatic muscle robot arm with MRB in order to improve the control performance with various external inertia loads.

From the experimental results, the damping torque of MRB was controlled by the applying magnetic field strength and the position control performance was improved without the decrease of response speed by separating the region where the damper produces a damping torque by phase plane switching control method.

In addition, to have optimal control parameters for the proposed phase plane switching control method, the neural network was used. The structure and leaning algorithm of neural network controller were very simple and applicable to any control system in order to minimize the position error.

From the experimental results, the newly proposed IPPSC was very effectively in high gain control with respect to the large external inertia load variation (0 to 10 Kg). And the steady state error with respect to various loads was reduced within ±1°.

References

Ahn, K. K., Lee, B. R. and Yang, S. Y., 2003, "Design and Experimental Evaluation of a Robust Force Controller for a 6-link Electro-hydraulic Manipulator Via H Infinity Control Theory," *In KSME Int. Journal*, Vol. 17, No. 7, pp. 999~1010.

Caldwell, D. G., Medrano-Cerda, G. A. and Goodwin, M., 1995, "Control of Pneumatic Muscle Actuators," *In IEEE on Control Systems Magazine*, Vol. 15, No. 1, pp. 40~48.

Caldwell, D. G., Razak, A. and Goodwin, M. J., 1993, "Braided Pneumatic Muscle Actuator," *IFAC Conf. on Int. Autonomous Vehicles*, Southampton, UK.

Caldwell, D. G., Tsagarakis, N., Medrano-Cerda, G. A., Schofield, J. and Brown, S., 1999, "Development of a Pneumatic Muscle Actuator Driven Manipulator Rig for Nuclear Waste Retrieval Operations," *In Proc. of the IEEE Int. Conf. on Robotics and Automation*, Vol. 1, No. 1, pp. 525~530.

Carbonell, P., Jiang, Z. P. and Repperger, D. W., 2001, "Nonlinear Control of a Pneumatic Muscle Actuator: Backstepping vs. Sliding-mode," *In Proc. of the IEEE Int. Conf. on Control Applications*, pp. 167~172.

Chan, S. W., John, H. L., Daniel, W. R. and James, E. B., 2003, "Fuzzy PD+I Learning Control for a Pneumatic Muscle," *In the IEEE Int. Conf. on Fuzzy Systems*, pp. 278~283.

Colbrunn, R. W., Nelson, G. M. and Quinn, R. D., 2001, "Modeling of Braid Pneumatic Actuators for Robotic Control," *In Proc. of the IEEE Int. Conf. on Intelligent robots and systems*, Vol. 4, No. 4, pp. 1964~1970.

Folgheraiter, M., Gini, G., Perkowski, M. and Pivtoraiko, M., "Adaptive Reflex Control for an Artificial Hand," *In Proc. of SYROCO 2003 Symposium on Robot Control*, Holliday Inn, Wroclaw, Poland.

Hesselroth, T., Sarkar, K., Van Der Smagt, P. P. and Schulten, K., 1994, "Neural Network Control of a Pneumatic Robot Arm," *In IEEE Trans. on Systems*, Vol. 24, No. 1, pp. 28~38.

Iskarous, M. and Kawamura, K., 1995, "Intelligent Control Using a Neural-Fuzzy Network," *In Proc. of the IEEE Int. Conf. on Intelligent Robot and System*, Vol. 3, No. 3, pp. 350~355.

Kishore, B. and Kuldip, S. R., 2003, "Fuzzy Logic

Control of a Pneumatic Muscle System Using a Linearizing Control Scheme," *In IEEE Int. Journal*, pp. 432~436.

Medrano-Cerda, G. A, Bowler, C. J. and Caldwell, D. G., 1995, "Adaptive Position Control of Antagonistic Pneumatic Muscle Actuators," *In Proc. of the IEEE Int. Conf. on Intelligent robots and systems*, Vol. 1, No. 1, pp. 378~383.

Noritsugu, T. and Tanaka, T., 1997, "Application of Rubber Artificial Muscle Manipulator as a Rehabilitation Robot," *In IEEE/ASME Transaction on Mechatronics*, Vol. 2, No. 4, pp. 259~267.

Noritsugu, T., Tsuji, Y. and Ito, K., 1999, "Improvement of Control Performance of Pneumatic Rubber Artificial Muscle Manipulator by Using Electrorheological Fluid Damper," *In Proc. of the IEEE Int. Conf. on Systems*, Vol. 4, pp. 788~793.

Osuka, K., Kimura, T. and Ono, T., 1990, "H∞ Control of a Certain Nonlinear Actuator," *In Proc. of the IEEE Int. Conf. on Decision and Control*, Vol. 1, pp. 370~371.

Tondu, B. and Lopex, P., 2000, "Modeling and Control of Mckbben Artificial Muscle Robot Actuators," *In IEEE Control System Magazine*, Vol. 20, No. 1, pp. 15~38.

Tsagarakis N., Caldwell, D. G. and Medrano-Cerda, G. A., 1999, "A 7 DOF Pneumatic Muscle Actuator (pMA) Powered Exoskeleton," *In Proc. of the IEEE Int. Workshop on Robot and Human Interaction*, pp. 327~333.

Van der Smagt, P. P., Groen, F. and Schulten, K., 1996, "Analysis and Control of a Rubbertuator Arm," Biol. Cybernetics, Vol. 75, pp. 433~440.

Yamada, T. and Yabuta, T., 1992, "Neural Network Controller Using Autotuning Method for Nonlinear Functions," *In IEEE Transaction on Neural Networks*, Vol. 3, pp. 595~601.